

Supporting Information

30 January, 2012

Ms. ID: ja-2011-09115e

**Site-Selective Cu Deposition on Pt Dendrimer-Encapsulated
Nanoparticles: Correlation of Theory and Experiment**

Emily V. Carino, Hyun You Kim, Graeme Henkelman, and
Richard M. Crooks

13 pages

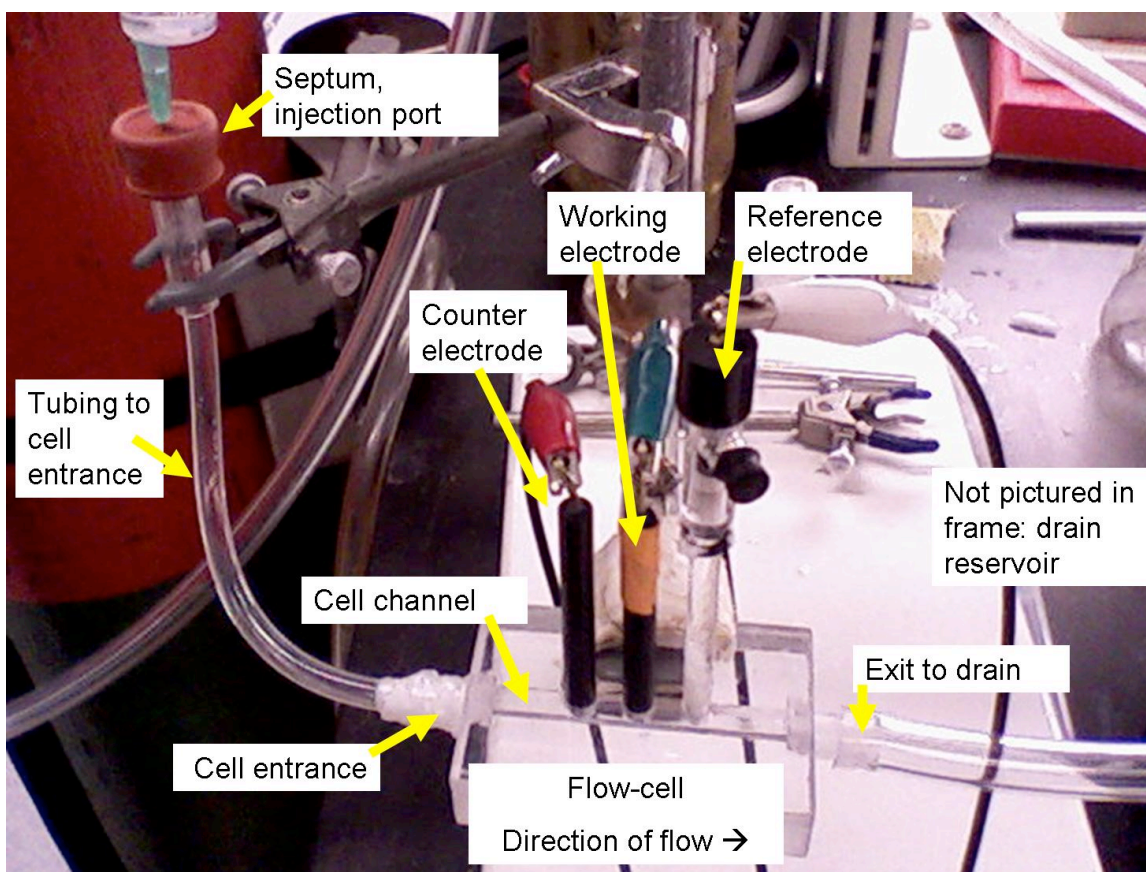


Figure S1. Photograph of the 3-electrode flow cell used for Cu UPD experiments on Pt DEN-modified electrodes. The cell is constructed from clear polycarbonate. The cell channel has a rectangular cross section and an internal volume of 1.0 mL, not including the volume of the tubing that attaches the cell entrance to the injection port. The electrodes (glassy carbon (GC) working, GC counter, and Hg/Hg₂SO₄ reference) insert into the channel via holes drilled through the top of the cell. The holes were precisely machined to the diameters of the electrodes to ensure air and water-tight seals. When fully inserted, the electrodes are coplanar with the interior cell wall. Electrolyte solutions are injected into the cell via a rubber septum at the injection port using a syringe having a 22 gauge needle. The injection port is connected to the entrance to the cell channel by Teflon tubing. The volume of this tubing is ~4 mL. All the solutions were purged with Ar for at least 10 min prior to being injected into the cell. The outlet empties into a glass container that is continuously purged with Ar to prevent backflow of O₂ into the cell.

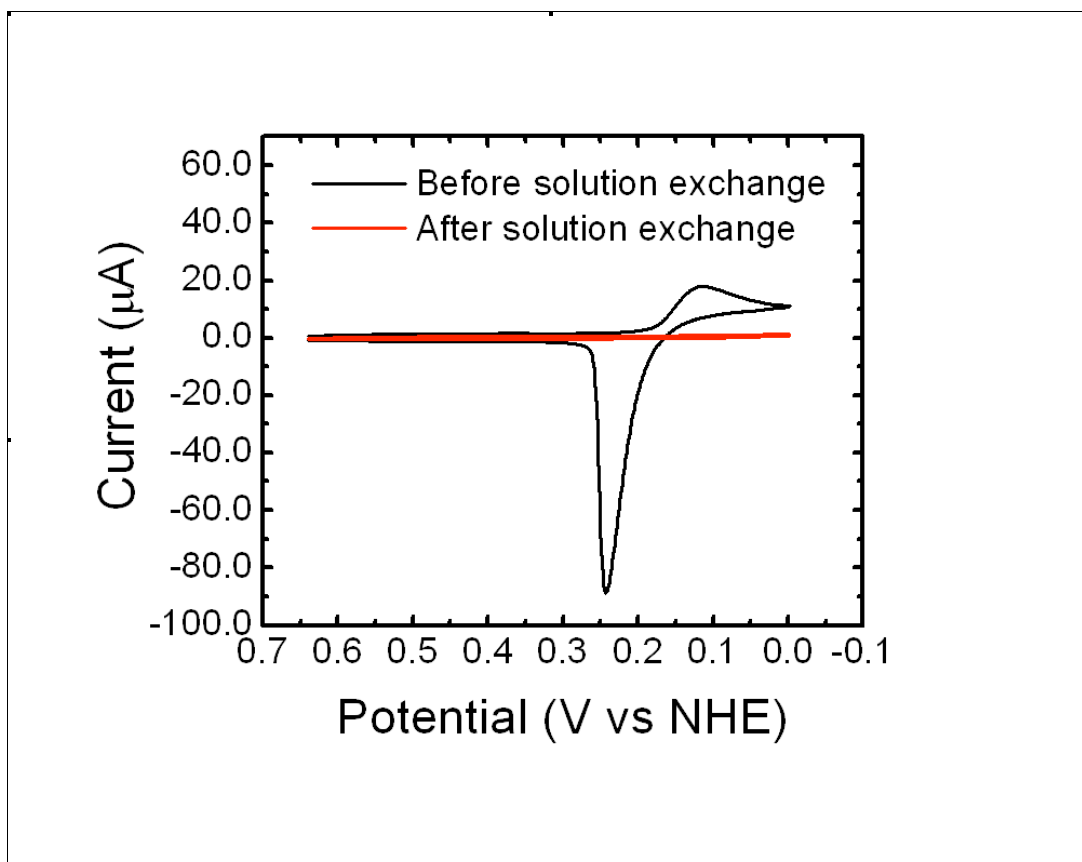


Figure S2. Cyclic voltammetry showing the results of a control experiment that demonstrates successful removal of Cu^{2+} from the flow cell (Figure S1). The black CV was recorded using a GC working electrode in a solution of Ar-purged, 0.10 M H_2SO_4 + 0.010 M CuSO_4 . The peaks correspond to the deposition and stripping of Cu. After recording the CV corresponding to the black line, the Cu^{2+} -containing solution was removed from the cell by rinsing it with 12.0 mL of Ar-purged, Cu^{2+} -free, 0.10 M H_2SO_4 . The red CV, which was recorded after the rinsing procedure, exhibits a featureless capacitance indicating the absence of Cu^{2+} . Both CVs began at 0.64 V and were initially swept in the negative direction at a scan rate of 100 mV/s.

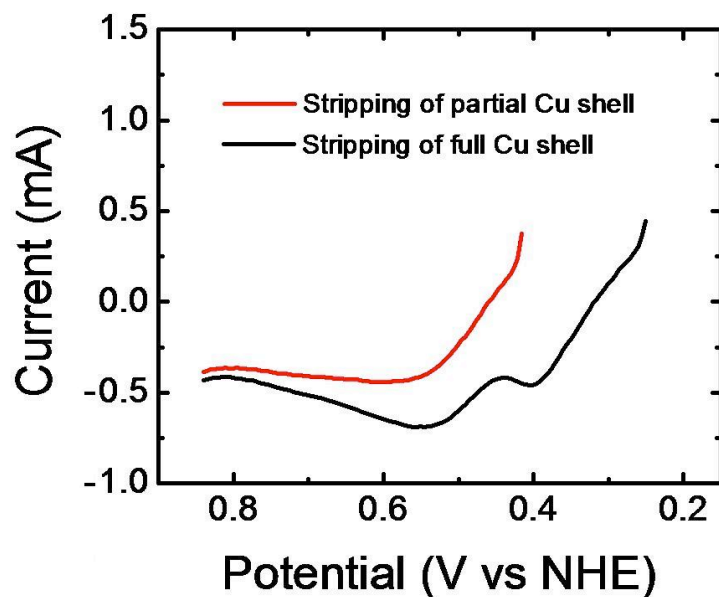


Figure S3. Linear sweep voltammograms corresponding to oxidation (stripping) of Cu from a G6-OH(Pt₁₄₇)-modified AvCarb working electrode. The data were obtained using the in-situ XAS cell. The current due to the stripping of a partial Cu shell from G6-OH(Pt₁₄₇@Cu_{Partial}) (red) exhibits only a single stripping wave. The current corresponding to the stripping of a full Cu shell from G6-OH(Pt₁₄₇@Cu_{Full}) (black) exhibits 2 stripping waves. The scan in red started at $V_{\text{Partial}} = 0.41$ V, was held at 0.41 V for 300 s, and was then swept in the positive direction. The scan in black started at $V_{\text{Full}} = 0.26$ V, was held at 0.26 V for 300 s, and was then swept in the positive direction. The scans were recorded at a scan rate of 2 mV/s in 0.10 M H₂SO₄ + 0.010 M CuSO₄ prior to collecting XAS spectra.

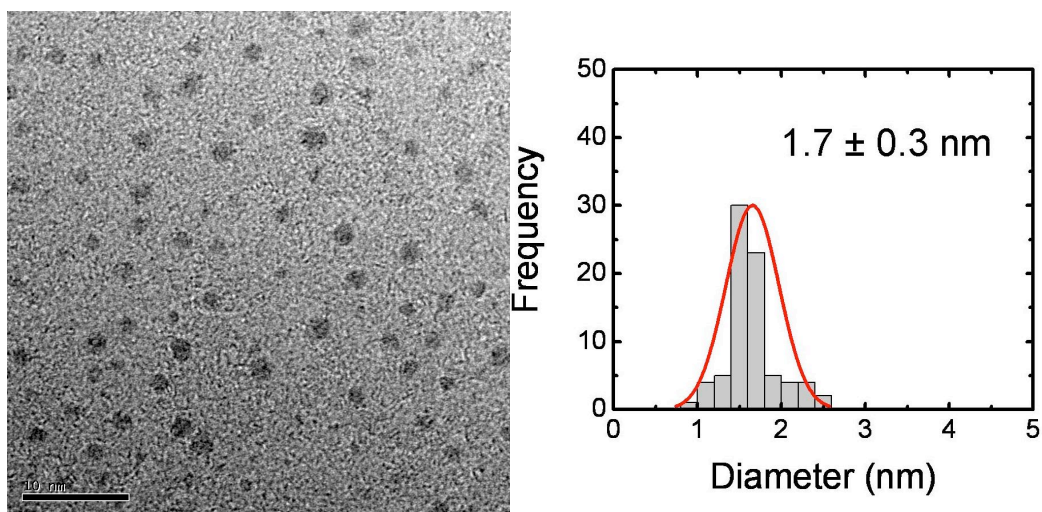


Figure S4. TEM micrograph of the G6-OH(Pt₁₄₇) DENs used in these experiments and the corresponding size distribution histogram.

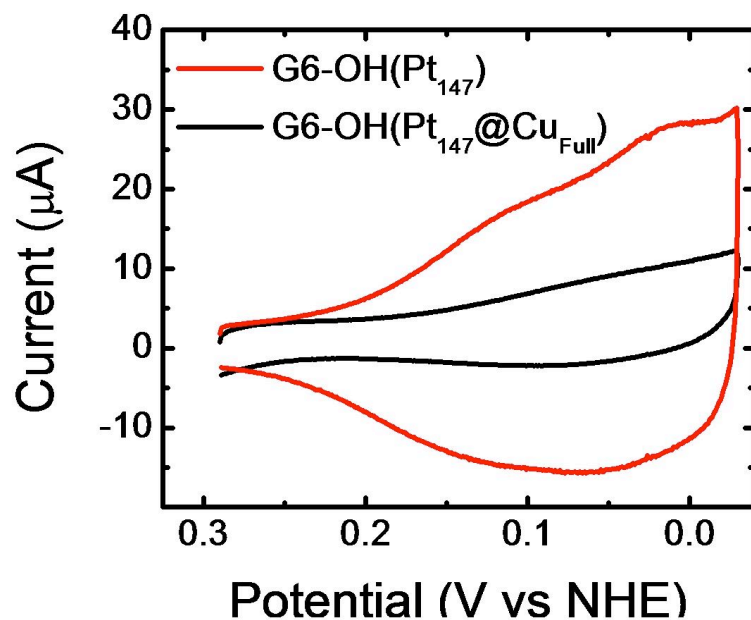


Figure S5a. Cyclic voltammograms of bare G6-OH(Pt₁₄₇) (red) and G6-OH(Pt₁₄₇@Cu_{Full}) (black) obtained in aqueous, Ar-purged 0.10 M H₂SO₄. The scans, which began at 0.29 V and were initially swept in the negative direction at a scan rate of 100 mV/s, cover the hydrogen evolution region (HER) and show that the presence of a full Cu UPD monolayer blocks most of the hydrogen activity of the Pt DENS.

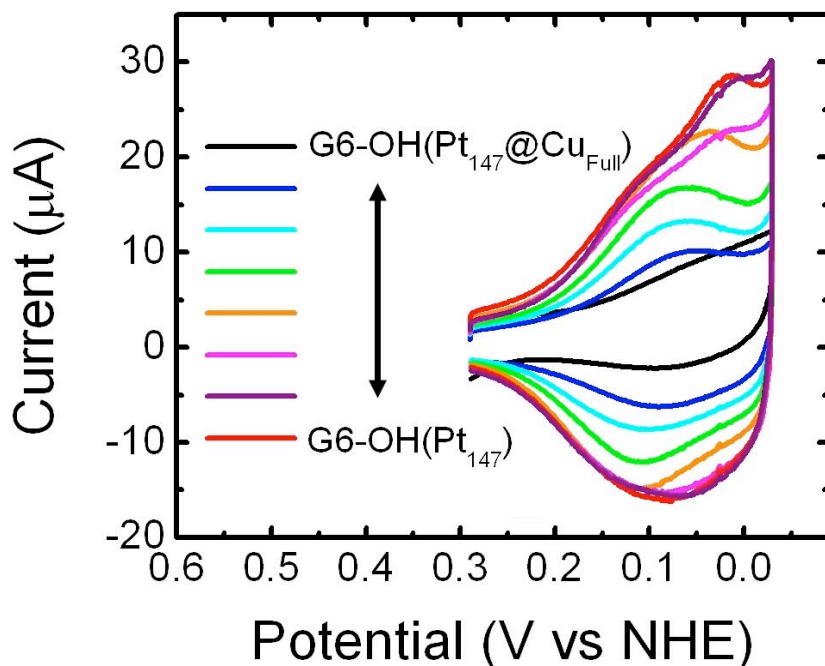


Figure S5b. CVs showing H_{UPD} on Pt DENs as the Cu coverage of the shell is incrementally decreased from full ($\text{G6-OH(Pt}_{147}\text{@Cu}_{\text{Full}})$) to bare Pt DENs ($\text{G6-OH(Pt}_{147})$). The CVs were recorded in Ar-purged 0.10 M H_2SO_4 at a scan rate of 100 mV/s. On bare $\text{G6-OH(Pt}_{147})$ (red line), two H_{UPD} waves are observed. We assign these to H_{UPD} onto different facets on the Pt DENs. On $\text{G6-OH(Pt}_{147}\text{@Cu}_{\text{Full}})$ (black line), the H_{UPD} waves are absent due to Pt being passivated by the Cu shell. When just small amounts of the Cu shell have been removed (dark blue, light blue, and green lines), only one peak in the H_{UPD} current is noticeable. When greater amounts of the Cu shell are removed (orange, pink, and purple lines), a second peak in the H_{UPD} current becomes apparent. This suggests that the removal of Cu and subsequent H_{UPD} takes place initially on only one of the two nanoparticle facets, while Cu remains on the other facet and is stripped last. This description accurately fits the DFT-calculated Cu stripping process.

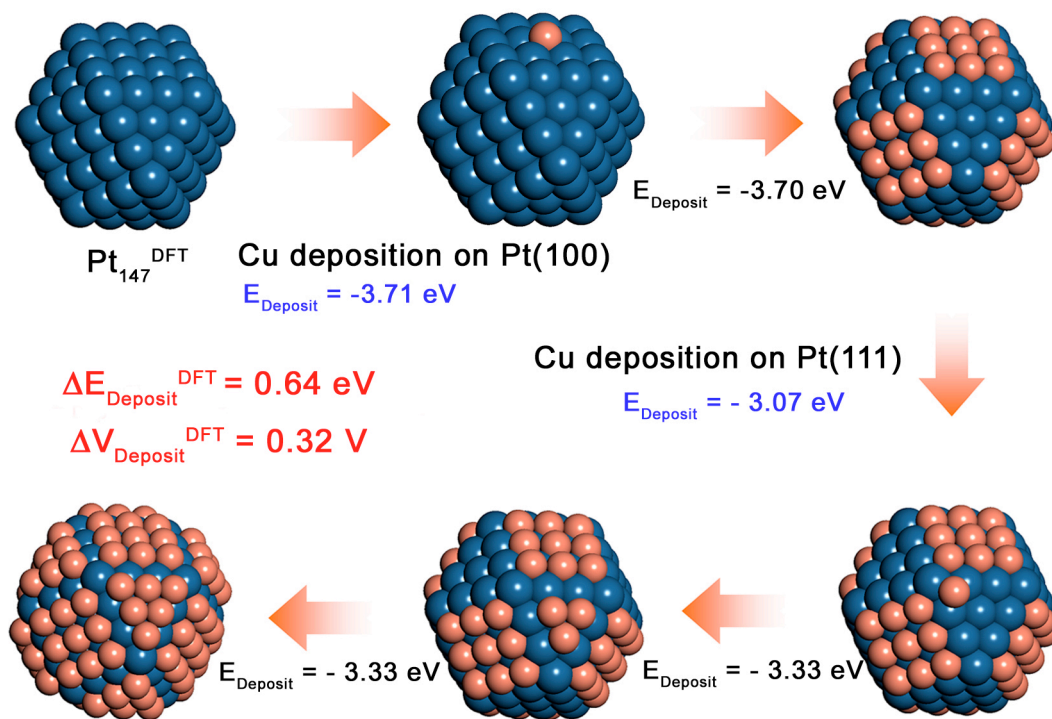


Figure S6. The detailed Cu deposition process on $\text{Pt}_{147}^{\text{DFT}}$. The E_{Deposit} values indicated by blue text were used to calculate the difference in potential between depositing Cu on different facets, $\Delta V_{\text{Deposit}}^{\text{DFT}}$.

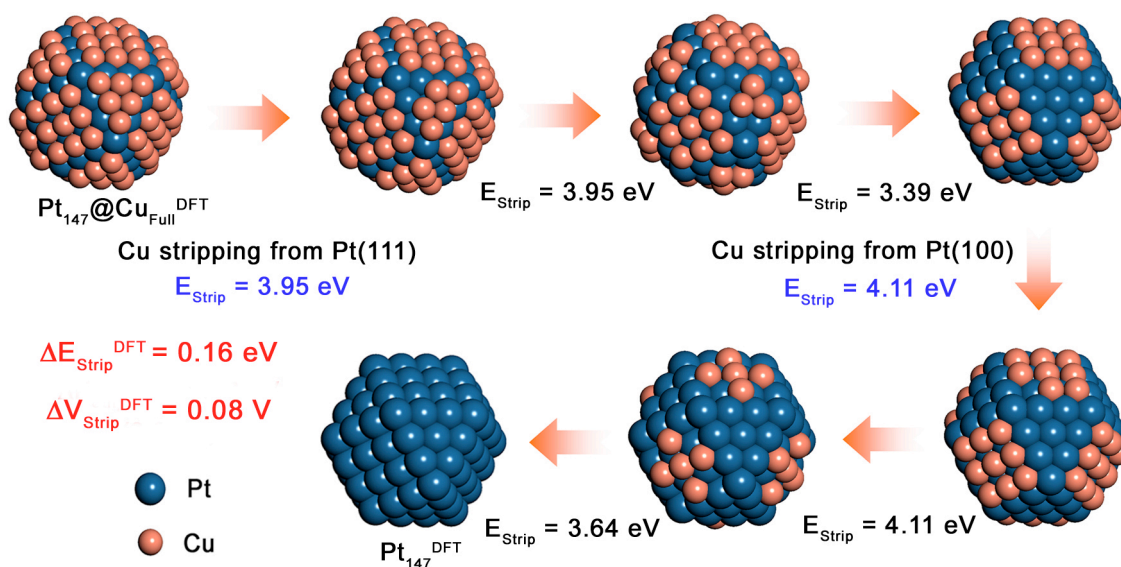


Figure S7. The complete process for Cu stripping from the $\text{Pt}_{147}@\text{Cu}_{\text{Full}}^{\text{DFT}}$ model. The E_{Strip} values given in blue indicate the peak generating steps.

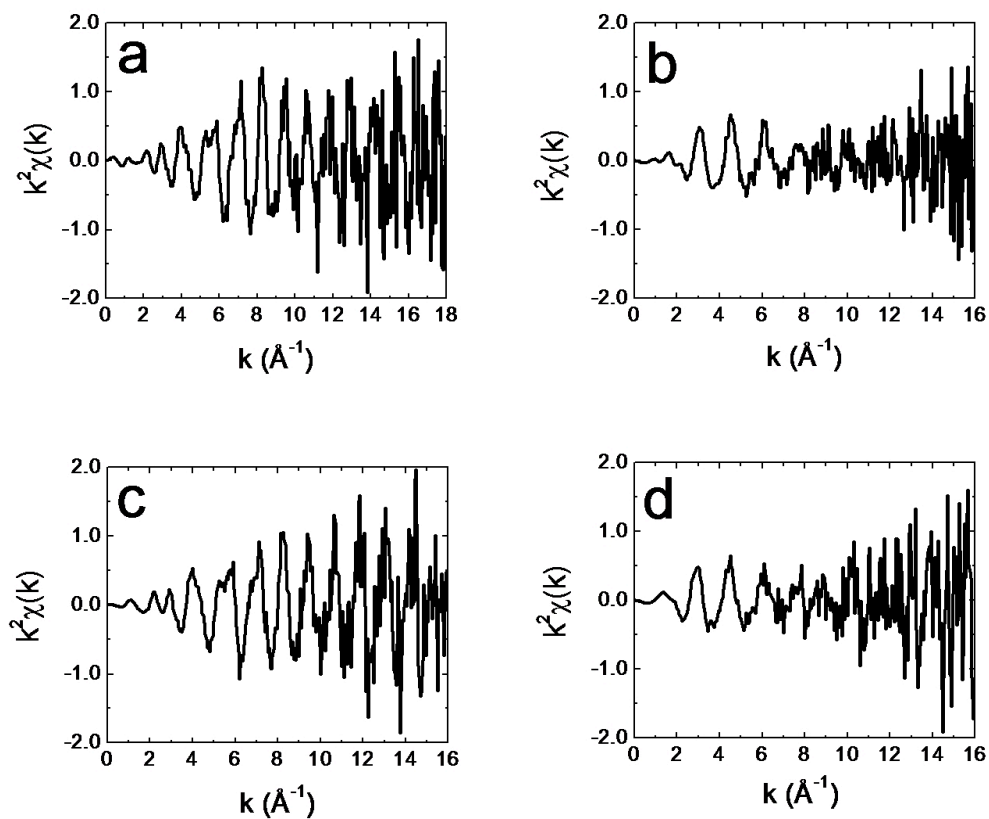


Figure S8. k-space data pertaining to the R-space distributions shown in Figure 7 for XAS data obtained from (a) the Pt edge of the G6-OH($\text{Pt}_{147}@\text{Cu}_{\text{Full}}$) DENSs; (b) the Cu edge of the G6-OH($\text{Pt}_{147}@\text{Cu}_{\text{Full}}$) DENSs; (c) the Pt edge of the G6-OH($\text{Pt}_{147}@\text{Cu}_{\text{Partial}}$) DENSs; and (d) the Cu edge of the G6-OH($\text{Pt}_{147}@\text{Cu}_{\text{Partial}}$) DENSs.

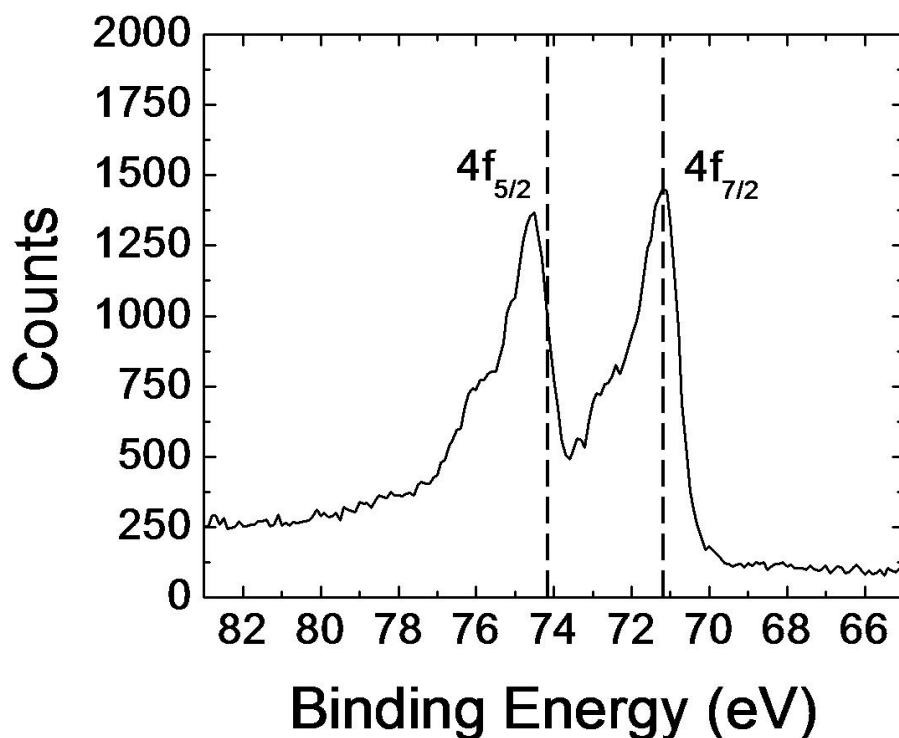


Figure S9. XPS data obtained from G6-OH(Pt₁₄₇) on AvCarb paper. The Pt 4f peaks are indicated for zerovalent Pt at 71.0 and 74.5 eV. The dashed lines correspond to the expected 4f values of zero-valent Pt: 71.2 and 74.2 eV.¹ The shoulders at 72.5 and 76.0 eV arise from the presence of some unreduced Pt²⁺ associated with the dendrimer.²

References

1. Wagner, C. D.; Riggs, W. M.; Davis, L. E.; Moulder, J. F. Handbook of X-Ray Photoelectron Spectroscopy; Perkin-Elmer Corporation: Chanhassen, MN, 1995.
2. Knecht, M. R.; Weir, M. G.; Myers, V. S.; Pyrz, W. D.; Ye, H.; Petkov, V.; Buttrey, D. J.; Frenkel, A. I.; Crooks, R. M. Synthesis and Characterization of Pt Dendrimer-Encapsulated Nanoparticles: Effect of the Template on Nanoparticle Formation. *Chem. Mater.* **2008**, *20*, 5218–5228.

Table S1. The bond distances and Debye-Waller factors extracted from the fit to the XAS data for G6-OH($\text{Pt}_{147}@\text{Cu}_{\text{Full}}$).

Coordination number (CN) ¹	Bond distance (Å)	Debye-Waller factor
n_{PP}	2.74	0.004 ± 0.0007
n_{PC}	2.65	0.023 ± 0.019
n_{CC}	2.68	0.005 ± 0.003
n_{CP}	2.65	0.023 ± 0.019
n_{CO} ²	1.98	0.06 ± 0.07
n_{Pm}	N/A ³	N/A
n_{Cm}	N/A	N/A

¹ CN is coordination number.

² n_{CO} represents Cu with a low-Z nearest-neighbor.

³ Not applicable (N/A) to n_{Pm} and n_{Cm} because these CNs are sums of other CNs and are not variables included in the fit.

Table S2. The bond distances and Debye-Waller factors extracted from the fit to the XAS data for G6-OH(Pt₁₄₇@Cu_{partial}).

Coordination number (CN) ¹	Bond Distance (Å)	Debye-Waller factor
n_{PP}	2.73	0.004 ± 0.0006
n_{PC}	2.56	0.010 ± 0.004
n_{CC}	2.63	0.019 ± 0.018
n_{CP}	2.56	0.010 ± 0.003
n_{CO} ²	1.98	0.004 ± 0.004
n_{Pm}	N/A ³	N/A
n_{Cm}	N/A	N/A

¹ CN is coordination number.

² n_{CO} represents Cu with a low-Z nearest-neighbor.

³ Not applicable (N/A) to n_{Pm} and n_{Cm} because these CNs are sums of other CNs and are not variables included in the fit.